https://doi.org/10.5281/zenodo.14843706

Techno-Economic Optimization of a Borehole Thermal Energy Storage and a District Heating System Using a New Open Data Framework for Integrated District Planning

Paul Mex
Fraunhofer Research Institution for Energy Infrastructures and Geothermal Systems (IEG)

Keywords: Borehole Thermal Energy Storage (BTES), Optimization, MILP, Simulation, District Energy Planning, District Heating Systems

Abstract

Sustainable district heating systems (DHS) will play a key role in the decarbonization of the heating sector in Germany and Northwestern Europe. When designing these complex systems, the interaction between producers, consumers, storages and the network must be optimized. Borehole thermal energy storages (BTES) are among the most promising seasonal storage solutions to address the asynchronous fluctuations of heat supply and demand. Mixed-integer linear programming (MILP) is a powerful approach for optimizing such DHS. This paper demonstrates the automated coupling of a non-linear BTES model with a techno-economic MILP optimization tool for DHS. For the BTES model, the open-source *python* tool *GHEDesigner*, based on the g-function approach, is chosen. It allows for the determination of the optimal number of boreholes and their optimal depth for given ground parameters while ensuring that the temperatures of the ground and the working fluid in the boreholes do not exceed predefined boundaries. So far, such detailed BTES models have primarily been used for isolated dimensioning or operational optimizations of single building energy systems or DHS neglecting the grid but focusing on the heat production site only. In our work, however, BTES are integrated into an optimization scheme for the design stage of an entire DHS including the grid. A case study demonstrates the automated creation of a DHS model based on publicly available data (Open Data) using the newly developed *Open District Hub* (*ODH*) planning framework developed in the *ODH@Jülich* project. This also includes the automated generation of load profiles for individual buildings. The system is dimensioned, simulated, and optimized, including a BTES system. This paper also includes a sensitivity analysis regarding important parameters such as soil thermal conductivity or drilling and electricity costs, which have a significant impact on the heat generation costs of the overall system.

1. Introduction

The Paris Agreement, established by the United Nations (UNFCCC, 2015), aims to reduce greenhouse gas emissions to limit global warming. The agreement sets a target to maintain the global average temperature increase well below 2 °C, with efforts to restrict it to 1.5 °C. Since 1981, the Earth's temperature has been rising at a rate of 0.18 K per decade, and the last 13 years have been the hottest ten years on record (Lindsey and Dahlmann, 2023). In Germany, approximately 30% of final energy consumption is attributed to space heating (25%) and hot water demand (5%). When considering process heat, heat accounts for 50% of Germany's total final energy consumption (AGEB, 2016; BMWK, 2021). This significant sector faces considerable challenges in achieving decarbonization. The success of the transition in the entire energy sector will mainly depend on the success of the transition in the heating sector.
80% of the energy supplied by German district heating systems (DHS) is based on fossil fuels (BMWK, 2019). Therefore, it is essential to decarbonize DHS through the integration of renewable

energy systems. Achieving this could position district heat as a crucial component in decarbonizing the overall heat supply in northwestern European countries, likely increasing its share in the energy mix (Lund *et al.*, 2010; Connolly *et al.*, 2014). One promising approach is the installation of large-scale central solar thermal collector (STC) fields (Schmidt *et al.*, 2004). To address seasonal energy fluctuations of supply and demand, storage systems must be integrated into these DHS. Currently, only sensible thermal energy storage (TES) systems are economically viable for large applications, as opposed to latent and chemical heat storage methods (Pinel *et al.*, 2011). Sensible TES can be classified into various types, including borehole (BTES), pit (PTES), tank (TTES), aquifer (ATES) and mine-water (MTES) thermal energy storage. The economic viability of BTES systems remains a subject of discussion (Yang *et al.*, 2021; Welsch, 2019). For optimizing DHS, mixed-integer linear programming (MILP) is a powerful approach. This paper presents the automated integration of a non-linear BTES model in a MILP techno-economic optimization tool for topologically discretized DHS called *Heatopia*, developed by Sporleder *et al.* (2024). In addition to that, a case study contributes to the aforementioned discussion on the economic viability of BTES. The case study has been set up using the tools from the *ODH@Jülich* framework in which *Heatopia* is integrated as well.

1.1 State-of-the-art

BTES consist of multiple ground heat exchangers (GHE). These GHEs are vertical boreholes fitted with a closed-loop piping system, commonly using U-, double-U-, or concentric pipe configurations. Water or glycol-water mixtures act as the working fluid circulating within these pipes. Heat is transferred between the soil and the working fluid primarily through conduction. Figure 1 shows the schematic design of a GHE.

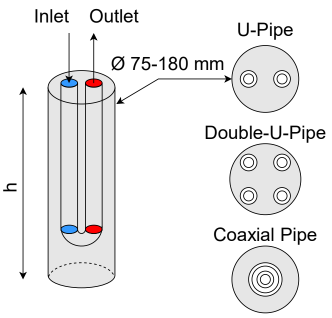

Figure 1: Representation of a GHE in heating mode. On the right-hand side, possible piping options are shown.

BTES are mostly simulated using analytical g-function approaches. Commercial software such as *EED* (Blocon AB, 2022) use pre-calculated closed source g-function-libraries. These are based on the work of Eskilson and Claesson who developed the *Superposition Borehole Model (SBM)* which is a closed source computer program to pre-calculate g-functions for given GHE fields (Eskilson, 1987; Eskilson and Claesson, 1988). Thus, only configurations that have already been pre-calculated and stored in that library can later be simulated, or interpolations between the g-functions have to be used.

As an alternative, the open source *python* package *pygfunctions* has been developed (Cimmino and Cook, 2022). It still permits the creation of pre-calculated libraries and enables rapid live calculations of g-functions for custom irregular GHE field configurations. *pygfunctions* facilitated the development of open-source GHE field optimization tools such as the *GHETool* (Peere and Blanke, 2022) and the *GHEDesigner* (Spitler *et al.*, 2022). Notably, the *GHEDesigner* is the only tool, among both open and closed source options, that can optimize both the depth and the layout of the field. The g-function approach can be directly implemented in MILP-models as long as the layout of the field is known and only the depth is unknown (Paly *et al.*, 2012; Beck *et al.*, 2013;

Gabrielli *et al.*, 2020; Kümpel *et al.*, 2022). However, the combination of an unknown GHE layout (or number of GHEs) and an unknown depth leads to a non-linearity which is why in the following an iterative coupling of the DHS MILP model and the BTES model using the *GHEDesigner* has been chosen.
This will facilitate the optimization of the design and operation of a BTES integrated into a large energy system, specifically a DHS that includes an STC field, a BTES heat pump (HP), and multiple consumers, as illustrated in Figure 2 and Figure 5. The optimization process simulates both the supply and demand units, as well as the grid. This study includes a sensitivity analysis to assess key parameters and their influence on the techno-economic performance of a BTES.
Following this introduction and a review of the current state-of-the-art of BTES modeling, the methods applied in this research will be outlined as well as the integration of the optimization in the *ODH@Jülich* framework for integrated district planning. In the results, the outcomes of the sensitivity analysis regarding parameters such as electricity prices, drilling costs and ground thermal conductivity will be presented. Finally, the results and findings will be discussed and concluded.

2. Methods

Heatopia is a MILP optimization tool for DHS (Sporleder *et al.*, 2024). It incorporates various components, including pipes, nodes, consumers, producers, thermal storages and technology constraints. The objective function seeks to minimize the cost function represented as $\min(f^{\text{opex,var}}, g^{\text{opex,fix}}, h^{\text{capex}})$. Here, $f^{\text{opex,var}}$ refers to the variable operational expenditures (opex) associated with storages or energy converters, encompassing costs related to energy carriers, maintenance and repair. Meanwhile, $g^{\text{opex,fix}}$ denotes the fixed opex for these systems. The term h^{capex} represents the capital expenditures. All costs are determined in accordance with VDI 2067 (VDI, 2012) using data from the Danish Energy Agency (2022) (in our case study for the year 2030). The analysis employs a ten-year time horizon, based on a one-year optimization at 24-hour time steps, with a conservatively estimated interest rate of 6% (ECB European Central Bank, 2024). The annuity factor α is calculated using equation (4) from VDI 2067 (VDI, 2012).

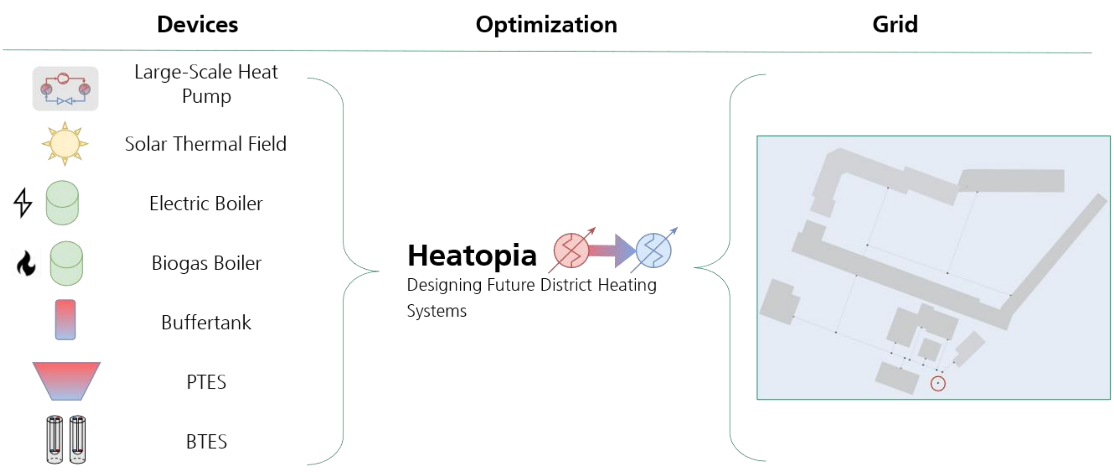

Figure 2: Visualization of the working principle of the MILP-Optimization tool *Heatopia*. It selects and dimensions the optimal devices from a set of possible devices (left). Furthermore, it optimizes all pipes of a topologically discretized network (right). The shown network is used for the case study below. The location of the production node is marked in red.

Figure 2 shows the working principle of *Heatopia* emphasizing that both the production devices (left) as well as the grid (right) are simulated and optimized. In previous studies, devices and the

grid have mostly been optimized separately (Bordin *et al.*, 2016; Wirtz *et al.*, 2021). The formulation as a MILP model enables us to not simulate certain fixed technology scenarios anymore but to pass an entire list of optional devices to the software tool. *Heatopia* then chooses and dimensions them with regards to the objective function.
The grid in Figure 2 and the demands have been created using the planning framework developed in the project *ODH@Jülich*. The concept of the framework is shown Figure 3.

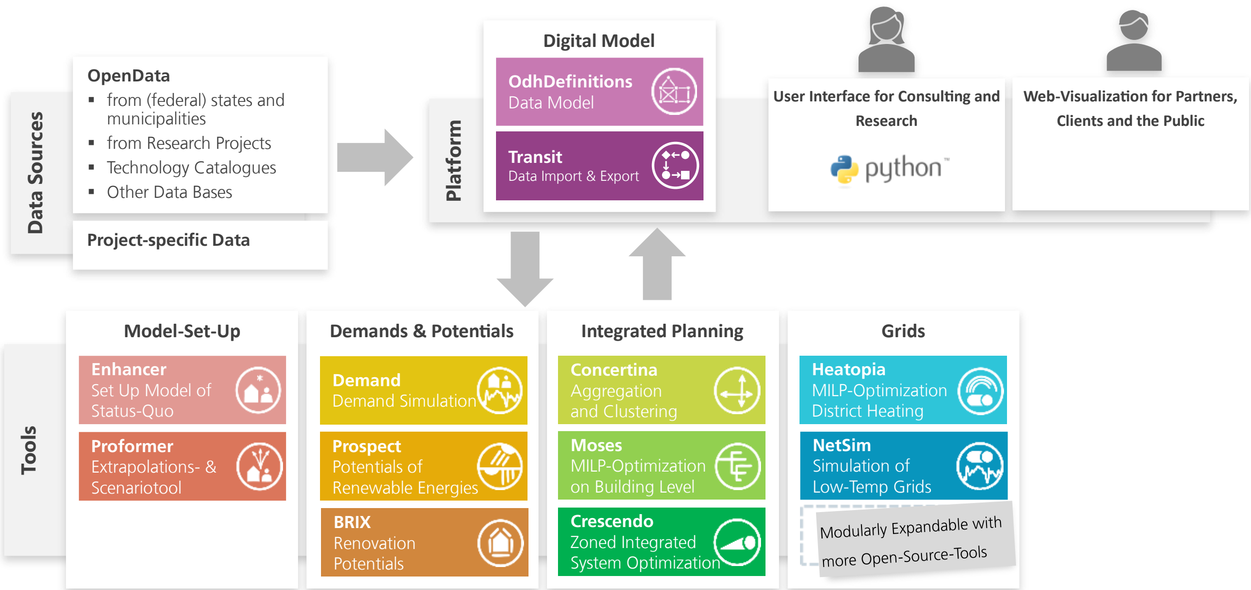

Figure 3: Visualization of the *ODH@Jülich* planning platform and central data model, its possible data sources and its tools. These tools are ordered from left to right in the order in which they might be used consecutively in a project.

In the *ODH@Jülich* project, several tools for integrated energy system planning as well as interfaces to public data sources, user interfaces and web visualization were developed. The entire platform is written in *python*. The central data model *OdhDefinitions* has been used to map all relevant building information, energy networks, energy systems and all other planning related data. It serves as the data backbone, ensures consistent data management and enables data exchange between all tools. Project-specific data can be enriched with additional public data sources and statistics. This provides the basis for demand estimations and assessments of renewable energy potentials. The developed user interface allows to define a polygon in a web-based interface to *OpenStreetMap (OSM)*. All buildings within the polygon are automatically identified and digital objects are created. The model was then merged with project data (including the grid in *GIS* format) and enhanced with public data sources and statistics (Statistische Ämter des Bundes und der Länder, 2011). Demands have been estimated using the *Demand* tool. The methodology to calculate the demands is based on the building information TABULA method (Loga and Diefenbach, 2013) and the Standardized-Load-Profile-Procedure implemented in *oemof* (Reiner Lemoine Institut, 2017). A more detailed presentation of the entire *ODH@Jülich* framework focusing on the *OdhDefinitions* module will be published soon and is not the scope of this paper.

2.1 Thermal simulation and integration of the BTES Model in the MILP optimization tool *Heatopia*

To integrate the BTES model into the DHS MILP optimization tool, a simplified storage model based on an energy balance is employed. This simplified model must already depict the typical techno-economic dynamics of a BTES. The algorithm is developed to identify the optimal heat flow entering $\dot{Q}^{\mathrm{in}}_{k=\mathrm{BTES},t}$ and exiting $\dot{Q}^{\mathrm{out}}_{k=\mathrm{BTES},t}$ the BTES with a resulting heat flow $\dot{Q}^{\mathrm{res}}_{k=\mathrm{BTES},t}$ which is

$$\dot{Q}^{\mathrm{res}}_{k=\mathrm{BTES},t} = \dot{Q}^{\mathrm{out}}_{k=\mathrm{BTES},t} - \dot{Q}^{\mathrm{in}}_{k=\mathrm{BTES},t} \text{ for } t \in Z^{\mathrm{time}}. \tag{1}$$

The energy balance of the BTES k at time t is

$$E_{k,t} = E_{k,t-1} + \Delta t\left(\dot{Q}^{\mathrm{in}}_{k,t} - \dot{Q}^{\mathrm{out}}_{k,t} - \dot{Q}^{\mathrm{loss}}_{k,t}\right) \text{ for } t \in Z^{\mathrm{time}}, k \in Z^{\mathrm{stor}}. \tag{2}$$

Here, Z^{time} represents the time set, and Z^{stor} denotes the set of all storages. All BTES losses per time step Δt are assumed to be $\dot{Q}^{\mathrm{loss}}_{k,t} = 0\ \mathrm{kW}$. This assumption results in a balanced profile of $\dot{Q}^{\mathrm{res}}_{k=\mathrm{BTES},t}$ over the course of one year. It implies that all thermal losses are offset by geothermal gains. All thermal energy taken from the ground will be reinjected in the same year. Common scenarios illustrating this can be found in the EED-Tutorials (EED, 2019) and are better considered as constraints rather than mere assumptions. Additionally, a cyclic condition is applied for all storages, stated as

$$E_{k \in Z^{\mathrm{stor}},t=0} = E_{k \in Z^{\mathrm{stor}},t=\mathrm{end}}, \tag{3}$$

where $E_{k \in Z^{\mathrm{stor}},t}$ is the energy level of the storage. The BTES is dimensioned with

$$\dot{Q}^{\mathrm{nom}}_{k} \leq \dot{q}^{\mathrm{nom,GHEs}}_{k} \cdot h_k \cdot z_k \text{ for } k \in Z^{\mathrm{BTES}}, \tag{4}$$

where the nominal dimension is $\dot{Q}^{\mathrm{nom}}_{k \in Z^{\mathrm{BTES}}} \leq \max\left(\dot{Q}^{\mathrm{res}}_{k \in Z^{\mathrm{BTES}},t \in Z^{\mathrm{time}}}\right)$ from Eq. (1) and $\dot{q}^{\mathrm{nom,GHEs}}_{k}$ is the specific nominal heat flow rate of a GHE in W m^{-1}. The variables z_k and h_k represent the number of GHEs and their depth, respectively. The investment costs for the BTES C^{inv}_{k} are expressed as

$$C^{\mathrm{inv}}_{k} \leq h_k \cdot z_k \cdot c^{\mathrm{drill}}_{k} \text{ for } k \in Z^{\mathrm{BTES}}, \tag{5}$$

where c^{drill}_{k} denotes the specific drilling costs in € m^{-1}, which is the primary investment cost factor for the BTES. The STC field and all heat pumps are simulated as in Sporleder *et al.* (2024).

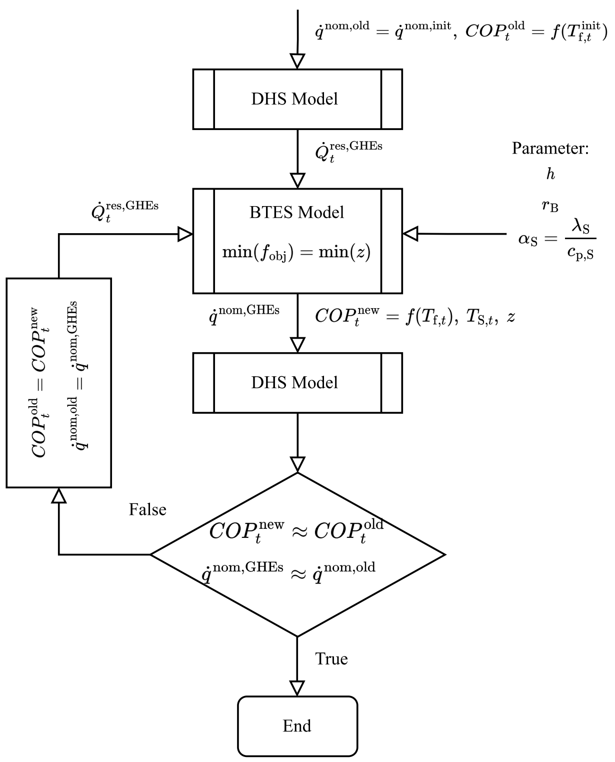

Figure 4: Flow chart showing the iterative coupling of the DHS model *Heatopia* and the BTES model

For the first run of the DHS optimization including all equations stated above, the $COP^{old}_{t} = COP_{k \in Z^{\mathrm{HP,BTES}},t}$ of the BTES heat pump is estimated (using an arbitrary sinus signal for the GHE working fluid temperature) as well as the nominal dimension of the GHEs $\dot{q}^{\mathrm{nom,init}}$ using soil parameters and tabular values from VDI 4640 (VDI, 2010). Then, as depicted in Figure 4, the optimal $\dot{Q}^{\mathrm{res}}_{k=\mathrm{BTES},t}$ is transmitted to the BTES model, in our case the *GHEDesigner*, which determines the optimal field layout of the BTES (including z_k and h_k), as well as the specific nominal heat flow rate $\dot{q}_k^{\mathrm{nom,GHEs}}$ and the working fluid temperature in the GHEs affecting $COP_{k\in Z^{\mathrm{HP,BTES}},t}$. These parameters are then returned to the DHS model. An iterative loop is established to address cases where the deviation of $\dot{q}^{\mathrm{nom,GHEs}}_{k\in Z^{\mathrm{BTES}}}$ and $COP_{t,k\in Z^{\mathrm{HP_{BTES}}}}$ before and after the iteration exceeds 6 % (being a relevant criterium only for $\dot{q}^{\mathrm{nom,GHEs}}_{k\in Z^{\mathrm{BTES}}}$ since the error of $COP_{t,k\in Z^{\mathrm{HP_{BTES}}}}$ has been observed to be always well below 1 %). Key parameters for the BTES model are, e.g., the radius of the GHE r_{B} and the thermal diffusivity α_{S} which is the fraction of the thermal conductivity of the soil λ_{S} and the volumetric heat capacity of the soil $c_{\mathrm{p,S}}$.

2.2 Case study and parameters

To assess the economic performance of a BTES combined with an STC field, we set up a case study for a small DHS and conducted a sensitivity analysis. The topology of the grid and the consumers is presented in Figure 2. The location is Karlsruhe, Germany. The combined consumers have a peak demand power of 0.6 MW and an annual energy demand of 1.2 GWh a^{-1}. A schematic overview of the devices at the production node is shown in Figure 5.

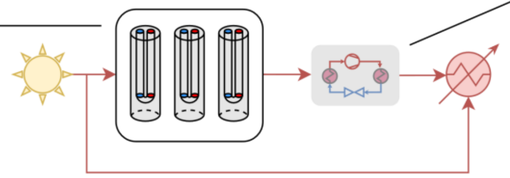

Figure 5: Devices at the production node of the case study system

The STC field can charge the BTES and/or feed directly the grid. The BTES is discharged via a large-scale heat pump to lift the temperature level to a forward flow temperature of 75 °C. For the sensitivity analysis, we varied the thermal conductivity λ_{S} and the specific drilling costs for the GHEs, both being key parameters for the BTES. Furthermore, we multiplied the dynamic electricity price profile by a constant factor of 1.5 and 2. For the base scenario we set $\lambda_{\mathrm{S}} = 2.5\ \mathrm{Wm^{-1}K^{-1}}$ equaling for example wet sand (Grünert *et al.*, 2009; SenStadt, 2018). The drilling cost were set to $c^{\mathrm{drill}} = 100\ €\mathrm{m}^{-1}$ (Robert and Gosselin, 2014; Blum *et al.*, 2011; Florides *et al.*, 2013). The electricity price profile is the wholesale electricity price projected for 2030. All other parameters have been chosen according to Mex and Sporleder (2024) and example number five in the EED tutorials (EED, 2019). The maximum depth of the BTES is set to 140 m.

3. Results

Heatopia calculates both constant optimized variables as well as dynamic ones being returned in an hourly resolution including operational data like the hourly power profiles of each producer and consumer. In the following sensitivity analysis, we will focus on constant key variables such as the overall heat generation cost (HGC). Figure 6 shows the optimized number of boreholes z and the overall HGC over a varied thermal conductivity between $\lambda_{\mathrm{S}} = 1.5\ \mathrm{Wm^{-1}K^{-1}}$ (being especially poor) and $\lambda_{\mathrm{S}} = 3\ \mathrm{Wm^{-1}K^{-1}}$ (very good). z decreases exponentially from over 60 to 42. The same exponential behavior can be observed regarding the HGC but within a much smaller range decreasing from about 22.4 to 20.9 ct/kWh.

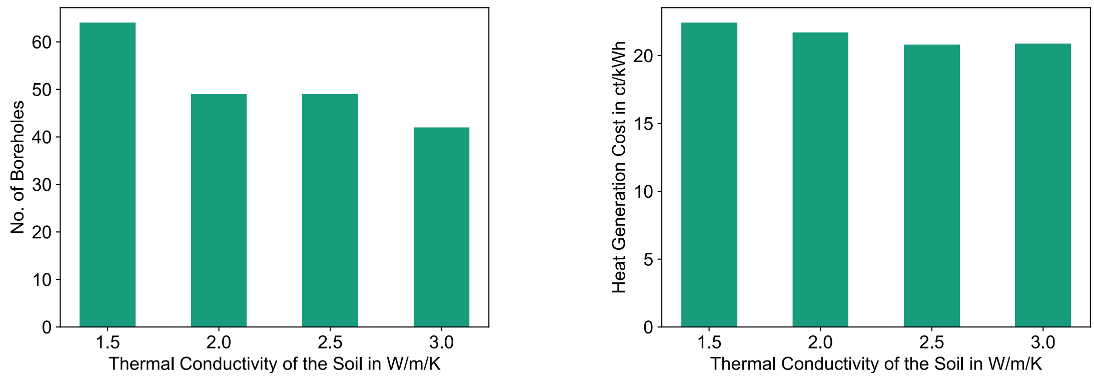

(a) (b)

Figure 6: Optimized number of boreholes of the BTES (a) and heat generation cost (b) over a varied thermal conductivity of the soil

Figure 7 plots the investments per device as well as the HGC over a varied specific drilling cost c^{drill}. Since the investments are coupled to the dimensions of the devices (linearly in the case of BTES and the STC field) their plot does also allow conclusions concerning the change of their dimensions over varied input parameters. For all different c^{drill}, the investments (and dimension) of the BTES heat pump remain constant at about 0.7 M€. Also, the STC field remains nearly unchanged. The dimension of the BTES itself remains constant, too, but the investments increase linearly as does c^{drill}. The HGC increase from 20.8 to 29.8 ct/kWh.

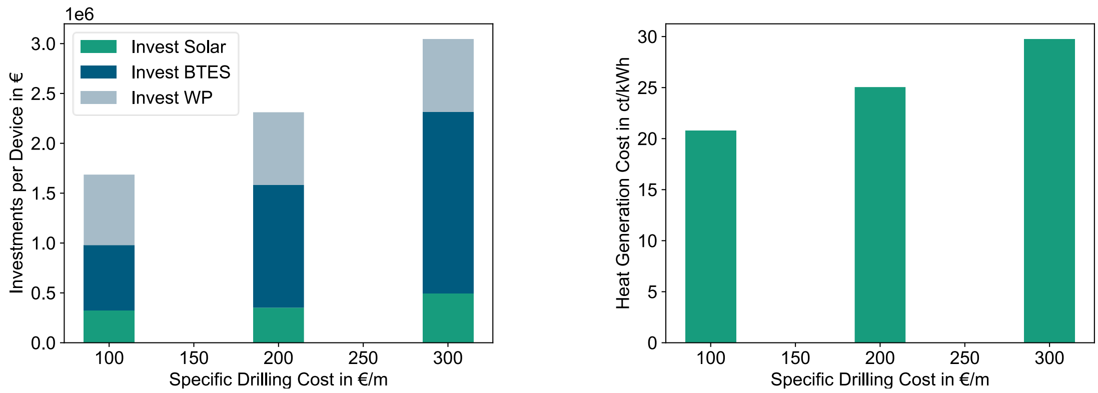

(a) (b)

Figure 7: Optimized investments per device (a) and heat generation cost over a varied specific drilling cost (b)

The development of the HGC and the investments per device over the electricity price are plotted in Figure 8. The HGC increase from 20.8 to 25 ct/kWh while the electricity price is doubled. In Figure 7, Figure 8 and Figure 9 the bar at the very left of the plots is associated with the base scenario. While for the base scenario electricity price profile the optimized investments for the STC field are 0.3 M€, they increase to about 0.8 M€ in case of a higher electricity price which also means that its optimal dimension is much larger. The investment for the BTES heat pump stays nearly constant at about 0.7 M€ while the investment for the BTES decreases slightly from 0.65 to 0.6 M€. Thus, the dimensions of the BTES decrease linearly by the same small factor.

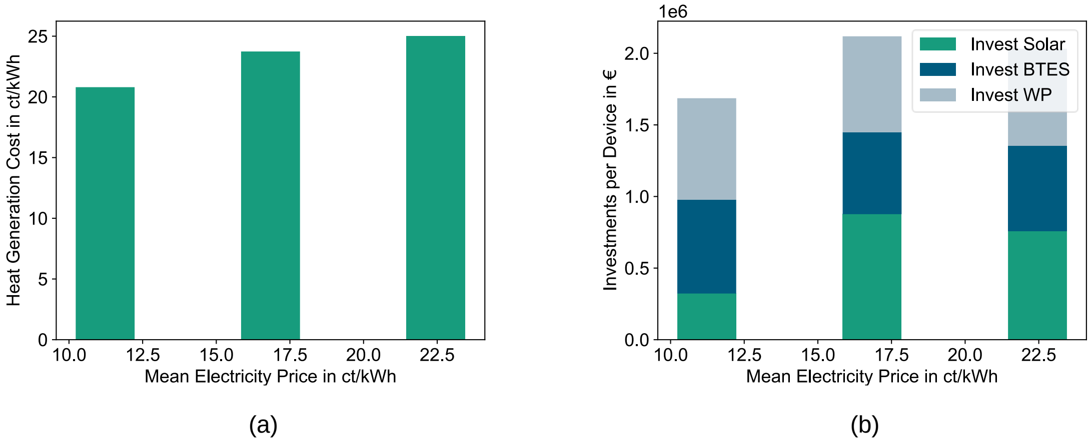

Figure 8: Optimized heat generation cost (a) and investments per device over a varied electricity price

The gross heat generation per device, in Figure 9 plotted over the electricity price, describes how much thermal energy is leaving a device. Since the output of the BTES is already depicted and equals the thermal input of the heat pump, we plotted in case of the heat pump only the electric input (which exits the heat pump together with the thermal input as thermal energy). The gross heat generation indicates how much energy is converted in a device, in other words, how much it is used.

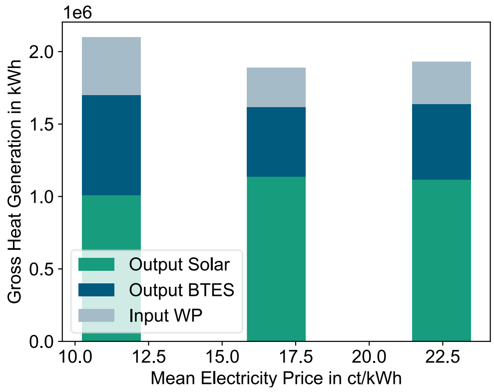

Figure 9: Gross heat generation per device over a varied electricity price. The gross heat generation of each device is the thermal energy leaving the device. For the heat pump, it is only the electric energy that is transformed into heat in the heat pump, since the output of the BTES is already depicted and equals the thermal input of the heat pump

For the STC field, 1.0 GWh is converted and used by the system in the base scenario while 1.1 GWh leave the device for scenarios with an increased electricity price. Note, that in these two scenarios, the dimension of the STC is much higher (see Figure 8) unlike the gross heat generation. Concerning the BTES and its heat pump, in the base scenario, 0.7 GWh thermal energy leave the BTES and 0.4 GWh of electric energy are transformed into heat within the BTES heat pump, these numbers decrease to 0.5 and 0.3 GWh in the case of a doubled electricity price.

4. Discussion

Regarding the influence of the thermal conductivity of the soil λ_S, our study shows a strong influence of λ_S on the number of GHEs z which decrease exponentially with an increasing λ_S. The same exponential behavior can be observed in the development of the HGC but with a very low gradient. Thus, z and its influence on the capex of the BTES have a comparably low impact on the

overall HGC. BTES systems can still be economically viable under rather poor conditions with respect to λ_{S}.
The specific drilling cost c^{drill} have a strong impact on the investment costs for a BTES (see Figure 7) which increase linearly with c^{drill}. This means that it is still economically more favorable to accept high investments in the BTES than increasing the STC field. The overall HGC increase from 20.8 to 29.8 ct/kWh. However, one should bear in mind that in Figure 7 c^{drill} is increased by 200 % which leads to a doubling of the accumulated investment costs of all devices. Nevertheless, at the same time the overall HGC increase by only less than 50 % indicating that the entire system HGC (based on a BTES and its heat pump and an STC field) are driven rather by the opex, not by the capex.
That is the reason why a sensitivity analysis of the electricity price is crucial since it means an altering of the opex conditions. Before, both for λ_{S} and c^{drill}, the HGC and total investments for the BTES changed, but the dimensions of all devices remained constant. However, when altering the electricity price (the opex conditions), the dimensions suddenly change dramatically. Due to the rather high temperature delta between the BTES and the grid, the COP of the BTES heat pump is rather low with values between 2 (for short periods of time) and 3.5, mostly being around 3. This leads to a high fraction of electric energy that is transformed into heat when using the heat pump leading to a high dependency on the electricity price. For an increased electricity price, it is economically more viable to install more STC capacity than using the heat pump. This increased capacity is also used for demand peaks. This conclusion can be drawn from the gross heat generation of the STC which increases by only 10 % while the investments and thus the dimension of the STC field is more than doubled (see Figure 8) from 1700 m^2 to 4000 m^2. This is also caused by the very low land area cost of only 15 €m^{-2} that we applied. Figure 9 shows, that while the usage of the STC increases, the usage of the BTES decreases by roughly a third. High electricity prices make the usage of BTES economically less favorable due to the low COP of the BTES heat pump. However, while the design changes strongly, the overall HGC increase moderately from 20.8 to 25 ct/kWh. Here, the optimum could be at a rather flat gradient, which is why in a real-world project a sensitivity analysis regarding the land area costs should be added at this point which might decrease the rather large, optimized dimension of the STC field. Furthermore, an additional renewable device only for peak loads could be worthwhile. It should be noted that Figure 8 (b) shows despite of further rising electricity costs a slight decrease of the investments for the STC field. This is a numerical effect caused by both the already mentioned very low gradient at the optimum and the error between the DHS and the BTES model which has even been lowered to 2 % for $\dot{q}^{\mathrm{nom,GHEs}}$ in this case. Since the number of GHEs z can only be an integer value, it might occur, at flat optimums, that it is $\Delta z = 1$ between the models. This shows the need for further research when coupling non-linear BTES models to MILP models. Another solution could be the direct implementation of a BTES model within a MILP DHS optimization tool, e.g., using the g-functions from the *Python* package *pygfunctions*, formulated in a way that would allow, depending on the application case, to optimize only either the number or the depth of the GHEs.

5. Conclusion and Outlook

The coupling of a BTES model to the MILP DHS optimization tool *Heatopia*, embedded in the *ODH@Jülich* planning framework, proved to be a powerful approach. It enables the user to optimize complex renewable DHS with a variety of variables. In a case study regarding the techno-economic performance of a BTES in combination with an STC field we could demonstrate, that the HGC of the overall system increase…

1. … slightly with the thermal conductivity of the soil.

2. … moderately with the electricity price.
3. … significantly with the specific drilling costs.

Dimensions and operation of the overall system depend substantially on the electricity price, thus on the opex and less on the capex conditions. This is caused by the rather low COP of the BTES heat pump due to the high temperature delta between the BTES and the grid. This could change in grids with a lower temperature such as 4th and 5th generation grids. The performance of BTES coupled to these grids could be the scope of future studies. In addition to that, the competition and interaction of photovoltaic and STC fields could be a subject to investigate, aiming to lower the dependency of BTES systems on the electricity price. Furthermore, in the discussion section we could identify the need for further research when coupling BTES to DHS models. In further research, this coupling approach could be extended to the coupling of other non-linear seasonal storage models like aquifer or mine-water storages.

References

AGEB, 2016, *Anwendungsbilanzen für die Endenergiesektoren in Deutschland in den Jahren 2013 bis 2015: Studie beauftragt vom Bundesministerium für Wirtschaft und Energie, Projektnummer: 072/15*, Arbeitsgemeinschaft Energiebilanzen e.V.

Beck, M., Bayer, P., Paly, M. de, Hecht-Méndez, J. and Zell, A., 2013, Geometric arrangement and operation mode adjustment in low-enthalpy geothermal borehole fields for heating, *Energy*, Vol. 49, pp. 434–443.

Blocon AB, 2022, *EED version 4: Update manual*, Lund, Sweden.

Blum, P., Campillo, G. and Kölbel, T., 2011, Techno-economic and spatial analysis of vertical ground source heat pump systems in Germany, *Energy*, Vol. 36 No. 5, pp. 3002–3011.

BMWK, 2019, *Energiedaten: Gesamtausgabe*, Berlin, Germany.

BMWK, 2021, Deutsche Klimaschutzpolitik, available at: https://www.bmwk.de/Redaktion/DE/Artikel/Industrie/klimaschutz-deutsche-klimaschutzpolitik.html#:~:text=Mit%20dem%20novellierten%20Gesetz%20wird,2045%20Treibhausgasneutralit%C3%A4t%20verbindlich%20erreicht%20werden.

Bordin, C., Gordini, A. and Vigo, D., 2016, An optimization approach for district heating strategic network design, *European Journal of Operational Research*, Vol. 252 No. 1, pp. 296–307.

Cimmino, M. and Cook, J.C., 2022, Proceedings of the IGSHPA Research Track 2022, in *Proceedings of the IGSHPA Research Track 2022, 2022*, International Ground Source Heat Pump Association.

Connolly, D., Lund, H., Mathiesen, B.V., Werner, S., Möller, B., Persson, U., Boermans, T., Trier, D., Ostergaard, P.A. and Nielsen, S., 2014, Heat Roadmap Europe: Combining district heating with heat savings to decarbonise the EU energy system, *Energy Policy*, Vol. 65, pp. 475–489.

Danish Energy Agency, 2022, Technology Data, available at: https://ens.dk/en/our-services/projections-and-models/technology-data (accessed 19 May 2023).

ECB European Central Bank, 2024, Euro area bank interest rate statistics: December 2023, available at: https://www.ecb.europa.eu/press/stats/mfi/html/ecb.mir2402~882b313998.en.html (accessed 23 May 2024).

EED, 2019, *Tutorial: Examples for EED v4*, Lund, Sweden.

Eskilson, P., 1987 (1987), Thermal Analysis of Heat Extraction Boreholes, PhD Thesis, Department of Mathematical Physics, University of Lund, Lund, Sweden, 1987.

Eskilson, P. and Claesson, J., 1988, Simulation Model For Thermally Interacting Heat Extraction Boreholes, *Numerical Heat Transfer*, Vol. 13 No. 2, pp. 149–165.

Florides, G.A., Christodoulides, P. and Pouloupatis, P., 2013, Single and double U-tube ground heat exchangers in multiple-layer substrates, *Applied Energy*, Vol. 102, pp. 364–373.

Gabrielli, P., Acquilino, A., Siri, S., Bracco, S., Sansavini, G. and Mazzotti, M., 2020, Optimization of low-carbon multi-energy systems with seasonal geothermal energy storage: The Anergy Grid of ETH Zurich, *Energy Conversion and Management: X*, Vol. 8, p. 100052.

Grünert, J., Kenkmann, T., Scheps, V., Pawlitzky, M., Scherf, B. and Ostin, A., 2009, *Nutzung von Erdwärme in Brandenburg: Heizen und Kühlen mit oberflächennaher Geothermie: Ein Leitfaden für Bauherren,* *Planer und Fachhandwerker,* 1st ed., Brandenburgische Energie Technologie Initiative (ETI), Potsdam, Germany.

Kümpel, A., Stoffel, P. and Müller, D., 2022, Development of a Long-Term Operational Optimization Model for a Building Energy System Supplied by a Geothermal Field, *J. Therm. Sci (Journal of thermal science)*, Vol. 31 No. 5, pp. 1293–1301.

Lindsey, R. and Dahlmann, L., 2023, Climate Change: Global Temperature, available at: https://www.climate.gov/news-features/understanding-climate/climate-change-global-temperature (accessed 11 October 2023).

Loga, T. and Diefenbach, N., 2013, *TABULA Calculation Method: Energy Use for Heating and Domestic Hot Water*, Reference Calculation and Adaptation to the Typical Level of Measured Consumption, Darmstadt, Germany.

Lund, H., Möller, B., Mathiesen, B.V. and Dyrelund, A., 2010, The role of district heating in future renewable energy systems, *Energy*, Vol. 35 No. 3, pp. 1381–1390.

Mex, P. and Sporleder, M., 2024, 37th International Conference on Efficiency, Cost, Optimization, Simulation and Environmental Impact of Energy Systems (ECOS 2024) - Internal Proceedings Preliminary Version, in ECOS 2024 (Ed.), *37th International Conference on Efficiency, Cost, Optimization, Simulation and Environmental Impact of Energy Systems (ECOS 2024) - Internal Proceedings Preliminary Version, Rhodes, Greece, 30.06.2024 - 05.07.2024*, ECOS 2024, Rhodes, Greece.

Paly, M. de, Hecht-Méndez, J., Beck, M., Blum, P., Zell, A. and Bayer, P., 2012, Optimization of energy extraction for closed shallow geothermal systems using linear programming, *Geothermics*, Vol. 43, pp. 57–65.

Peere, W. and Blanke, T., 2022, GHEtool: An open-source tool for borefield sizing in Python, *Journal of Open Source Software*, 7(76) No. 4406.

Pinel, P., Cruickshank, C.A., Beausoleil-Morrison, I. and Wills, A., 2011, A review of available methods for seasonal storage of solar thermal energy in residential applications, *Renewable and Sustainable Energy Reviews*, Vol. 15 No. 7, pp. 3341–3359.

Reiner Lemoine Institut, 2017, oemofopen energy system modelling framework, available at: https://reiner-lemoine-institut.de/oemof/ (accessed 10 November 2024).

Robert, F. and Gosselin, L., 2014, New methodology to design ground coupled heat pump systems based on total cost minimization, *Applied Thermal Engineering*, Vol. 62 No. 2, pp. 481–491.

Schmidt, T., Mangold, D. and Müller-Steinhagen, H., 2004, Central solar heating plants with seasonal storage in Germany, *Solar Energy*, Vol. 76 No. 1, pp. 165–174.

SenStadt, 2018, *Geothermisches Potenzial - spezifische Wärmeleitfähigkeit und spezifische Entzugsleistung (Ausgabe 2018)*, Berlin, Germany.

Spitler, J., West, T. and Liu, X., 2022, Proceedings of the IGSHPA Research Track 2022, in *Proceedings of the IGSHPA Research Track 2022, 2022*, International Ground Source Heat Pump Association.

Sporleder, M., Rath, M. and Ragwitz, M., 2024, Solar thermal vs. PV with a heat pump: A comparison of different charging technologies for seasonal storage systems in district heating networks, *Energy Conversion and Management: X*, Vol. 22, p. 100564.

Statistische Ämter des Bundes und der Länder, 2011, Endgültige Ergebnisse der Gebäude- und Wohnungszählung 2011.

VDI, 2010, *Thermal use of the underground: Fundamentals, approvals, environmental aspects No.* 4640, VDI Verein Deutscher Ingenieure, Berlin, Germany.

VDI, 2012, *Wirtschaftlichkeit gebäudetechnischer Anlagen: Grundlagen und Kostenberechnung* 2067 Blatt 1.

Welsch, B., 2019 (2019), Technical, Environmental and Economic Assessment of Medium Deep Borehole Thermal Energy Storage Systems, Dissertation, Department of Material and Earth Sciences, Technische Universität Darmstadt, Darmstadt, Germany, 2019.

Wirtz, M., Hahn, M., Schreiber, T. and Müller, D., 2021, Design optimization of multi-energy systems using mixed-integer linear programming: Which model complexity and level of detail is sufficient?, *Energy Conversion and Management*, Vol. 240, p. 114249.

Yang, T., Liu, W., Kramer, G.J. and Sun, Q., 2021, Seasonal thermal energy storage: A techno-economic literature review, *Renewable and Sustainable Energy Reviews*, Vol. 139, p. 110732.

Acknowledgement
This research has been funded via the project *ODH@Jülich*.

Gulbener Straße 23, 03046 Cottbus, Germany
paul.mex@ieg.fraunhofer.de